FISEVIER

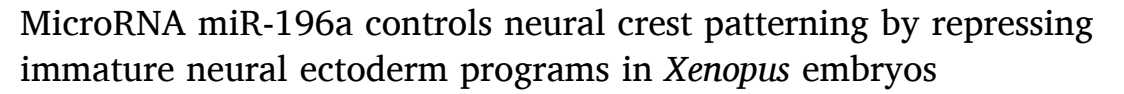
Contents lists available at ScienceDirect

Developmental Biology

journal homepage: www.elsevier.com/locate/developmentalbiology



Original research article



Alice M. Godden ^a, Nicole Ward ^a, Méghane Sittewelle ^{b,c}, Marco Antonaci ^a, Rafeeq Mir ^a, Aleksandr Kotov ^{b,c}, Anne H. Monsoro-Burq ^{b,c,d,1}, Grant N. Wheeler ^{a,*,1} ^o

- ^a School of Biological Sciences, University of East Anglia, Norwich Research Park, Norwich, NR4 7TJ, United Kingdom
- b Université Paris-Saclay, Département de Biologie, Faculté des Sciences d'Orsay, Signalisation Radiobiology and Cancer, CNRS UMR 3347, INSERM U1021, Orsay, F-91405. France
- ^c Institut Curie Research Division, Paris Science et Lettres Research University, Orsay, F-91405, France

ARTICLE INFO

Keywords:
microRNAs
miR-196a
Neural crest
BMP signalling
Neural induction
Pluripotency
Xenopus laevis and tropicalis embryos
Dorsal ectoderm gene regulatory networks

ABSTRACT

Neural crest (NC) cells form a multipotent stem cell population specified during neurulation, which undergo an epithelial-to-mesenchymal transition (EMT) and migrate extensively in the developing embryo, to generate numerous tissues and cell types including the craniofacial skeleton, the peripheral nervous system and pigment cells. The genetic and molecular details of NC specification are governed by a complex, yet still partially understood gene regulatory network (NC-GRN). In particular, the precise function of microRNAs (miRNA) in this network remains poorly characterized. MiRNAs are short non-coding 20–22 nucleotides long RNAs, which control gene expression through post-transcriptional repression. Since miRNA-196a is expressed in the developing neural and NC cells of *Xenopus laevis* embryos, we here investigated miR-196a function in the NC-GRN, by knocking-down its expression using antisense morpholinos. Depletion of miR-196a revealed major NC and craniofacial phenotypes. These defects were preceded by the perturbed expression of key neural, neural border and NC markers such as sox2/3, sic1/3, pax3, sox10 and snail2. Using RNA sequencing of individual neural border and NC explants, we have identified a signature of genes up- and down-regulated by miR-196a and validate these with rescue experiments using a miRNA mimic. Our study identifies miR-196a as a key actor of early patterning in the dorsal ectoderm, balancing the extent of immature neural plate progenitors with NC and placode specification, while also promoting neuron differentiation within the neural plate.

1. Introduction

MicroRNAs (miRNAs) are short, single-stranded, non-coding RNAs, of approximately 22 nucleotides long (Alberti and Cochella, 2017; Lee et al., 1993; Shah et al., 2017). They act mainly as repressors of gene expression by binding to the untranslated region at the 3' end of a targeted mRNA and either promoting the stalling of the ribosome or directly promoting the degradation of the targeted mRNA. They can be found either in intronic regions of the genome, processed from the introns allowing for co-expression of the miRNA and coordinating protein (Salim et al., 2022), or as independent genes from which many miRNA precursors can be produced in one transcript and then processed individually (Thatcher et al., 2008). MiRNAs are highly conserved in

evolution and are found in both plants and animals (Bartel, 2004). It was reported that 60 % of protein-coding genes in humans have conserved target sites for miRNAs (Friedman et al., 2009). In particular, miRNAs play important roles in the development of invertebrates like the worm and fruit fly (Chandra et al., 2017) and of vertebrates, including chick, mouse, frog and fish (Ahmed et al., 2015; Lewis and Steel, 2010; Mok et al., 2017; Thatcher et al., 2008; Ward et al., 2018). Some miRNAs regulate neural development (Yapijakis, 2020) and different steps of neural crest (NC) formation (Antonaci and Wheeler, 2022; Weiner, 2018).

Neural and NC progenitors are induced in the dorsal ectoderm of vertebrate embryos concomitantly with the positioning of the axial and paraxial mesoderm under the ectoderm. The dorsal ectoderm is patterned into three main territories, the neural plate (NP) in the

 $\textit{E-mail addresses:} \ anne-helene.monsoro-burq@curie.fr \ (A.H.\ Monsoro-Burq), \ grant.wheeler@uea.ac.uk \ (G.N.\ Wheeler).$

^d Institut Universitaire de France, Paris, F-75005, France

^{*} Corresponding author.

 $^{^{1}}$ co-last authors.

Abbreviations

EMT epithelial-to-mesenchymal transition

HG hatching gland MO morpholino miRNA microRNA

MM mismatch morpholino

NB neural border NC neural crest

NNE non-neural ectoderm NPB neural plate border

WISH whole mount in situ hybridisation

midline, the adjacent neural border (NB) and the non-neural ectoderm (NNE) laterally (Pla and Monsoro-Burq, 2018). The NP will form the central nervous system, while the NNE participates in skin external layers. Between these two territories, the NB domain includes progenitors for the dorsal-most NP cells, the hatching gland progenitors in frogs and the NC cells and cranial placodes (Betancur et al., 2010; Godden et al., 2021; Pla and Monsoro-Burq, 2018; Steventon and Mayor, 2012). Fate decisions in the dorsal ectoderm are controlled by finely tuned spatial-temporal modulations of BMP, WNT and FGF signalling (Alkobtawi et al., 2021).

From NB progenitors, pre-migratory NC cells form from gastrulation to neurulation and end up at or close to the developing neural folds. They exit from the dorsal epithelium by a stereotypical EMT, and migrate towards multiple locations of the embryonic body, where they differentiate into many differentiated cell types and tissues. The NC forms neurons and glia of the peripheral sensory, autonomous and enteric nervous system, the craniofacial skeleton and mesenchyme, the adrenal medulla chromaffin cells, and pigment cells (Aoto et al., 2015; Cheung and Briscoe, 2003). These discreet fates depend on the origin of the cells along the body axis, on the diversity of programs elicited prior to emigration, on signals encountered along the migration paths and on niches and environmental signals at the destination (Sauka-Spengler and Bronner-Fraser, 2008). Any errors in these processes can result in neurocristopathies, a large group of congenital disorders where aberrant NC migration, specification, or differentiation leads to multiple defects in NC derivatives (Gouignard et al., 2016; Ward et al., 2018). Some neurocristopathies correlate with dysregulation of miRNA expression, suggesting that miRNAs may be therapeutic targets for these disorders (Bachetti et al., 2021; Evsen et al., 2020; Pilon, 2021; Schoen et al., 2017). Previous research has identified how Wnt signalling can lead to repression of let-7 miRNA activity in avian NC cells (Bhattacharya et al., 2018). In avian models it has also been found that NC cells express high levels of DICER, important for processing and biogenesis of miRNAs. These miRNAs were then found to target parts of the FGF signalling pathway which is critical in neural induction in amniotes (Copeland and Simoes-Costa, 2020). We have previously characterised the expression of miRNAs in early Xenopus development (Ward et al., 2018) and examined miRNAs that potentially play a role in NC development (Godden et al., 2021, 2023; Ward et al., 2018). However, despite some progress little is still know regarding the role of specific miRNAs in NC development. Here, we find that miR-196a is required for NC development in Xenopus laevis embryos, and that its depletion in cranial NC strongly impairs craniofacial skeleton formation.

2. Results and discussion

2.1. miRNA 196a is essential for neural crest-derived craniofacial development

We previously characterised miR-196a expression in Xenopus

embryos during late gastrula and neurula stages (Godden et al., 2021; Ward et al., 2018). To assess miR-196a function in NC development two antisense morpholino (MO) oligonucleotides were designed, one complementary to the mature Xenopus laevis miRNA (miR-196a-MO), the other as a mismatch control containing 5-mismatched residues (miR-196a-MM, Table 1). MO binding to the miRNA prevents it from interacting with its target mRNAs (Flynt et al., 2017). The miR-196a-MO efficiently decreased miR-196a expression in a dose-dependent fashion as shown by qPCR while the miR-196a-MM had no effect, compared to un-injected control samples (Fig. S1A). MO miR-196a-MO is complementary to both miR-196a and -b isoforms, however we showed effective rescue of miR-196a KD with addition of miR-196a mimic, but we do not rescue loss of miR-196b, therefore the rescue experiment is isoform specific to miR-196a (Fig. S1D-F). Injection of miR-196a-MO leads to craniofacial phenotypes, although mild, that can be seen externally on stage 28 tadpoles, with asymmetric branchial arches (Fig. 1B). Moreover, miR-196 downregulation caused by miR-196a-MO was rescued by co-injection of a Xenopus tropicalis (xtr) miR-196a mimic, a synthetic RNA oligonucleotide mimicking xtr-miR-196a (Fig. S1D-G). The miR-196a mimic alone did not have a developmental phenotype (Fig. S1C). Together these data demonstrate the efficiency and the specificity of our in vivo depletion strategy.

We next assessed the developmental phenotypes resulting from unilateral depletion of miR-196a, the various approaches used are illustrated in Fig. 1A. At stage 28, control tadpoles present a welldeveloped head and facial bulges where the NC populates the branchial arches (Fig. 1B arrows). On the injected side, both control and miR-196a-MM-injected tadpoles formed craniofacial structures normally. In contrast, the tadpoles injected with miR-196a-MO lacked the branchial mesenchyme structures (Fig. 1B) as observed when NC cells are ablated (Milet et al., 2013). The other parts of the larvae were overall well developed, albeit a small size reduction (Fig. 1, Fig. S1B). This phenotype remained until the end of embryonic development, indicating that it was not due to a delay in craniofacial morphogenesis. Alcian blue-stained cartilages of stage 42 morphant tadpoles showed a phenotype on the injected side, with reduced and poorly differentiated cartilaginous branchial arches structures (Fig. 1C, arrow), and missing Meckel's and palatoquadrate cartilages. Midline skeletal structures remained unchanged. In other parts of the body, NC-derived melanocytes and fin mesenchyme seemed normal (Fig. S1C). These results match CRISPR/Cas9 knockdown of miR-196a (Godden et al., 2021) and indicate that miR-196a plays a major role in NC development, especially for its ectomesenchymal cranial derivatives, prompting us to explore further at which stage the NC-GRN may be affected.

2.2. miRNA-196a regulates dorsal ectoderm patterning

To investigate at which developmental stage miR-196a affected the

Table 1
Comparison of miR-196a vs miR-196b sequences in relation to designed MO
Sequences obtained from miRbase (http://www.mirbase.org/). Mature miRNA

sequence is highlighted in bold.

MiRNA	Sequence 5'-3'	Genomic location
miR-196a Accession number: MI0004942	UAGGUAGUUUCAUGUUGUUGG	chr2: 142905363–142905468 [-]
miR-196b Accession number: MI0004943	UAGGUAGUUUUAUGUUGUUGG	chr6: 32896531–32896617 [+]
miR-196a MO	CAATCCCAACAACATGAAACTACCT	-
miR-196a MM miR-196a LNA mimic	ATTGCCAAGAACATCAAAGTACCT UAGGUAGUUUCAUGUUGUUGGG	-

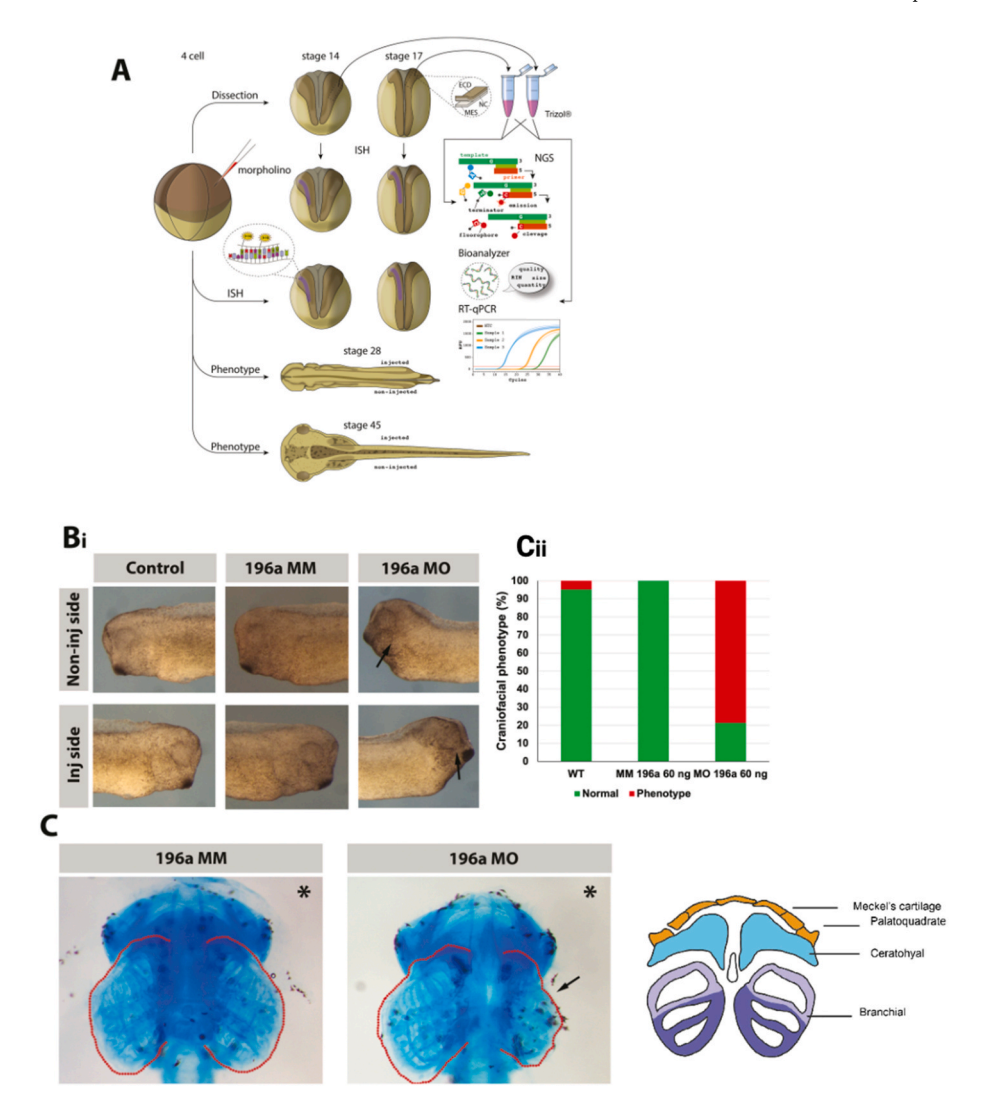


Fig. 1. Depletion of miR-196a impairs neural crest-derived craniofacial development (A) Experimental paradigm for RNA sequencing of single NB or NC explants. Embryos were injected into one dorsal blastomere at the 4-cell stage of development. All embryos were co-injected with 5 ng GFP capped RNA. (B) Craniofacial phenotypes seen in tadpoles are indicated by arrows (stage 28), phenotype observed in 15/18 embryos. (C) Alcian blue cartilage preparations show clear branchial arch and cartilage phenotypes on the injected side following miRNA-196a KD (stage 45). (Cii) The graph shows blind count data for alcian blue phenotype analysis for: wild type, mismatch miR-196a MO and miR-196a MO. Test used for statistical analysis is Chi-squared on independent repeats, miR-196a MM vs MO p=1.3348e-08. (For interpretation of the references to colour in this figure legend, the reader is referred to the Web version of this article.)

development of NC or its surrounding tissues, whole mount in situ hybridisation for the main early markers of each fate was carried out on unilaterally injected morphant embryos (Figs. 2 and 3). At NP stage (stages 13-15) or neural fold stage (stages 16-18), depletion of miR-196a led to a loss of expression for the NC markers snai2, sox10 and the NB marker pax3 while miR-196a-MM did not affect gene expression compared to the control un-injected side (Fig. 2, Fig. S2). Interestingly pax3 expression was reduced in early neurula stage embryos (Fig. 2 and Fig. 2) but then appeared more disorganised in later mid-neurula stage embryos (Fig. S2). We further explored neural and NB formation. We found that NP (sox2, sox11) and NP/NB markers (zic1/3) were expanded, while the lateral NB marker msx2 was absent from anterior NB (Fig. 3, Fig. S3 A-C). Pax6 was slightly expanded in the eye progenitor domain and reduced in the NP territory, while notch-responsive Hairy1 gene was decreased in both domains (Fig. 3). miR-196a is located within an intron of the hoxC9 gene (Godden et al., 2021). Anterior-posterior patterning was therefore probed using engrailed2 (en2) which marks the mid-hindbrain boundary: either a slight posterior shift or lack of expression was observed in morphant neural tissue (Fig. 3, Fig. S3 A and B), suggesting an anteriorisation of the morphant neural domain at neural fold stage. This is consistent with the observed expansion of pax6-positive eye domain and recess of pax6 spinal cord domain (Fig. 3). Importantly, the specificity of these phenotypes was confirmed by rescuing the MO phenotype using injection of miR-196 mimic on snai2, sox10 (NC) and pax3 (NB) (Fig. S2). For all markers no phenotype was seen following injection of embryos with either control miRNA mimic (cel-miR-39-3p), miR-196a mimic, or mismatch 196a-MM alone (Fig. 2 and Fig. S3 A and B). Collectively, these results indicate perturbation of dorsal ectoderm patterning upon depletion of miR196a. Imbalanced expression of essential NB specifiers is known to result in failure of NC formation in favour of adjacent neural or non-neural tissue development (de Croze et al., 2011). Here we observe a failure of activation for the key transcription factors of the NB-NC-GRN pax3, msx2, snai2, and sox10 (Figs. 2 and 3). Neural progenitors are expanded, especially anteriorly (marked by sox2, sox11, pax6, zic1/3), however, we observed that neuronal differentiation was impaired at the end of neurulation as differentiation markers tubb2b (formerly N-tub) and elrC were decreased on the morphant side (Fig. 3). At later tailbud

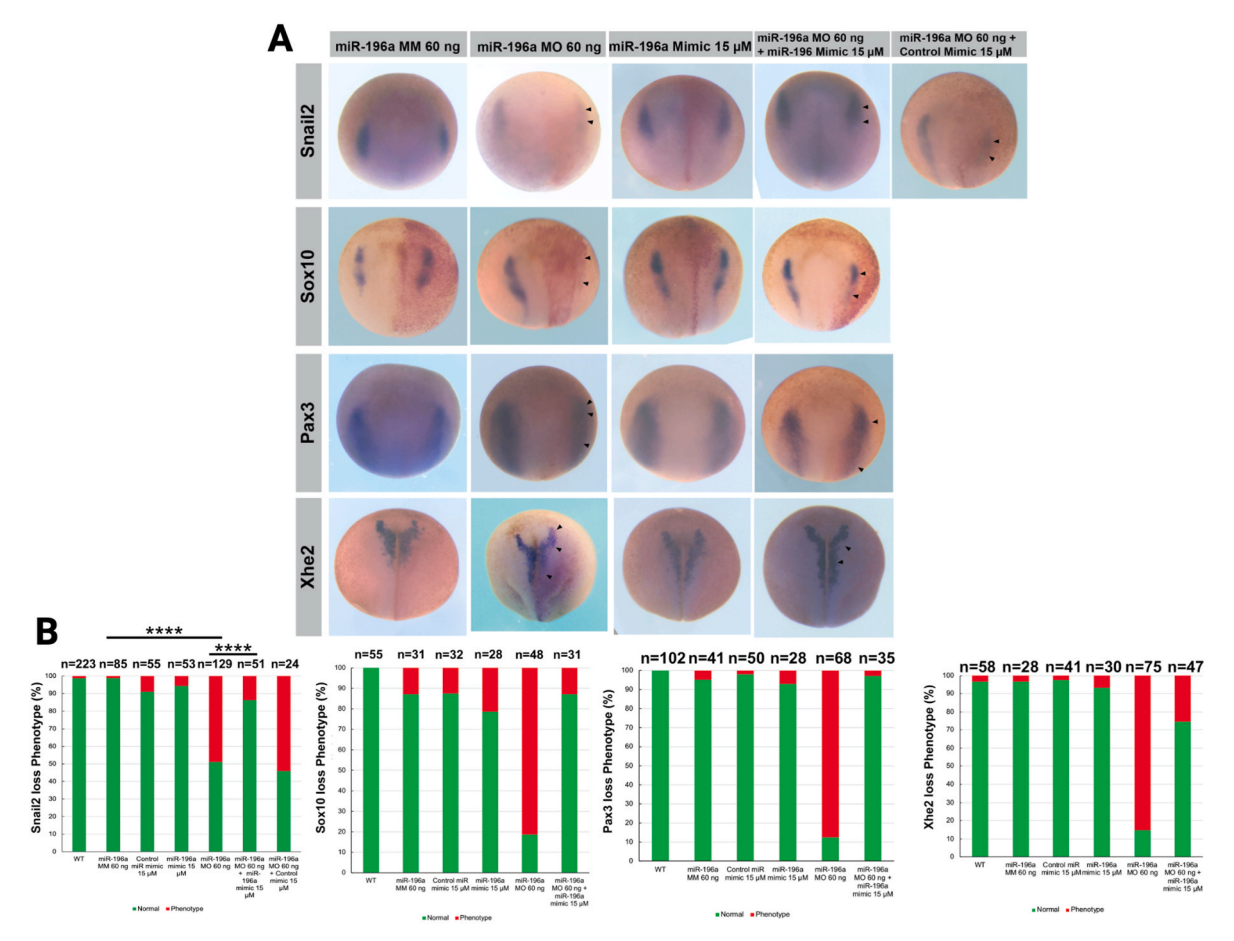


Fig. 2. Functional characterisation of MO mediated miRNA KD and rescue with synthetic miRNA on development of NC, NPB and HG in developing *X. laevis* embryos. MiRNA KD led to HG, NC and NPB phenotypes. Embryos were injected into one dorsal blastomere at the 4-cell stage of development with 300 pg of lacZ cRNA as a tracer, developed with red-gal. Injected side is always right side. WISH of snail2 (st. 14), sox10 (st. 14), pax3 (st. 14), pax3 (st. 14) and Xhe2 (st. 15) following miR-196a MO mediated knockdown. Black arrowheads indicate regions of phenotypic interest. (A) MiR-196a morpholino KD phenotypes for NC, NPB, and HG. with control groups: miR-196a MM and miR-196a MO and mimic rescue (B) Count data for phenotype incidence. Control miRNA mimic (cel-miR-39-3p). Chi squared statistical testing was carried out on Snail2 data, as three independent experiments were conducted covering 3 biological repeats and many technical repeats. between MM MO and MO and mo and mo and rescue group. For miR-196a MM MO vs MO $p = 4.72 \times 10^{-14}$, for miR-196a MO vs rescue p = 0.000013. (For interpretation of the references to colour in this figure legend, the reader is referred to the Web version of this article.)

stages of development (st. 27) expression of NC factors was decreased. Fig. S4 shows expression of twist1 is lost in the NC in miR-196a morpholino injected embryos. Similar results were seen for sox10 (not shown).

2.3. Transcriptomes of miR-196a morphant NC progenitors indicate loss of NC and placodes, expansion of immature neural programs and aberrant BMP/Notch signalling

Using RNA sequencing, we compared micro-dissected NB at NP stage (stage 14) with pre-migratory NC at neural fold stage (stage 17), after 196-MO or 196-MM injections (Fig. S5). The ectoderm layers were taken, while the underlying mesoderm was avoided, as in (Plouhinec et al., 2017). Accuracy of the dissection was tested by probing the donor embryos with *pax3* for NB and *snai2* for NC, after dissection (Fig. S5A and B). PCA analysis of the triplicates indicates grouping of the samples according to their injection type (Fig. S5C and D). In addition, correlation analysis confirmed that the transcriptomes of control samples were grouped according to developmental stage and together, while the morphant transcriptomes were grouped separately (Fig. 4A). Interestingly, stage 17 morphant samples grouped closer to the control stage 14, raising the possibility that the phenotype could resemble a developmental delay. However, our phenotype analysis at later neurula stages using *twist1* as a NC marker (Fig. S4) and using alcian blue staining of st.

45 tadpoles (Fig. 1) indicates that any potential delay is not compensated later, as also shown in other experimental settings where NC development is delayed during neurulation (Figueiredo et al., 2017).

We used tissue expression signatures from single cell data to define the expression profile of landmark genes (Kotov et al., 2024; Petrova et al., 2024). A dot plot represents the intensity and percent of positive cells expressing a given gene in a cell type at different developmental stages (ectoderm, eye, NB, NC, neural ectoderm, neurons, NNE, NP and placodes) and illustrates the promiscuity of gene expression (Fig. 4B). Among the 2432 genes differentially expressed in NB explants at NP stage 14, the NC markers snai2, sox8, sox9, tfap2b, c3 and twist1 were depleted (Fig. 4C) while at that stage, NP markers remained little changed (e.g. sox2, zic1). In contrast, at the end of neurulation, in NC explants that should be ready to undergo EMT and cell migration, the morphant NC cells exhibited aberrant high expression of early NP markers sox2/3 and of pluripotency genes ventx2.2 (nanog ortholog) and its target pou5f3 (oct4 ortholog) (Fig. 4D). Those genes are essential for earlier steps of NC progenitor formation but should be downregulated at that stage (Scerbo and Monsoro-Burq, 2020).

We further explored ectoderm patterning processes using significantly differentially expressed genes from RNA-seq data and comparing early and late neurulation stages (Fig. 5B, Fig. S6B). It is known that neural crest development relies upon carefully balanced expression levels of a series of TFs. Here, we found that key TFs that establish the

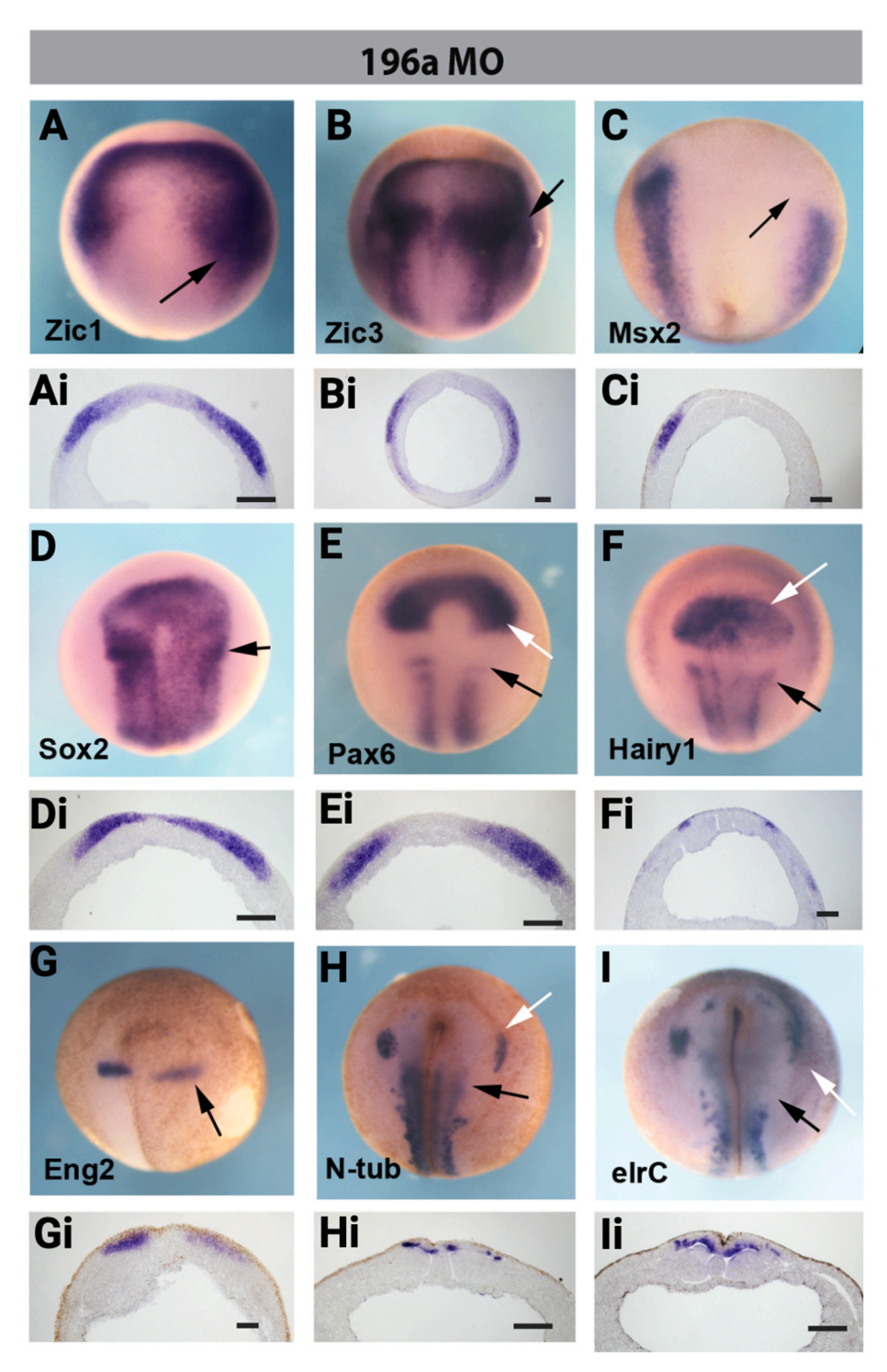


Fig. 3. Depletion of miR-196a expands neural plate progenitors at the expense of neural crest specification and neuronal differentiation. Embryos were injected into one dorsal blastomere at the 4-cell stage of development with 300 pg of GFP mRNA or of lacZ developed with Red-gal. In all panels the injected side is to the right. Whole mount *in situ* hybridisation of *zic1*, (stage 14), *zic3*, (stage 14), *msx2*, (stage 14), *pax6*, (stage 15) *hairy1*, (stage 18), *eng2*, (stage 15) *n-tub* (stage 18) and *elrc1*, (stage 18), following MO mediated miRNA KD. Embryos are positioned in dorsal view with anterior at the top. Wholemounts are shown as well as transverse sections (i). Injection of the MO caused an expansion in the NPB markers Zic1 (n = 28/30) and Zic3 (n = 34/37) but a loss in the anterior region of the NPB marker Msx2 (n = 18/19) (A–C). The neural marker Sox2 was expanded in a lateral direction and appeared to lose the intense dark region of expression seen in the control side (see black arrow) (n = 37/37) (D). Expression of the neural marker Pax6 was slightly enlarged across the anterior neural fold (lens primordia) (see white arrow) but reduced in the position of the forebrain stripe (see black arrow) (n = 18/24) (E). The downstream target of Notch – Hairy1 had a reduced but broadened expression (n = 22/25) (F) Eng2 showed a reduced and broadened expression as well as a shift more posterior (n = 19/25) (G). Both neuronal differentiation markers N-tub (n = 24-30) and ELRC (n = 23/24) were reduced following miR-196aMO injection although this was restricted to the anterior most part of the NP (see black arrows). The expression of these two markers in the trigeminal placodes had extended in both an anterior and posterior direction (see white arrows) (H,I). (For interpretation of the references to colour in this figure legend, the reader is referred to the Web version of this article.)

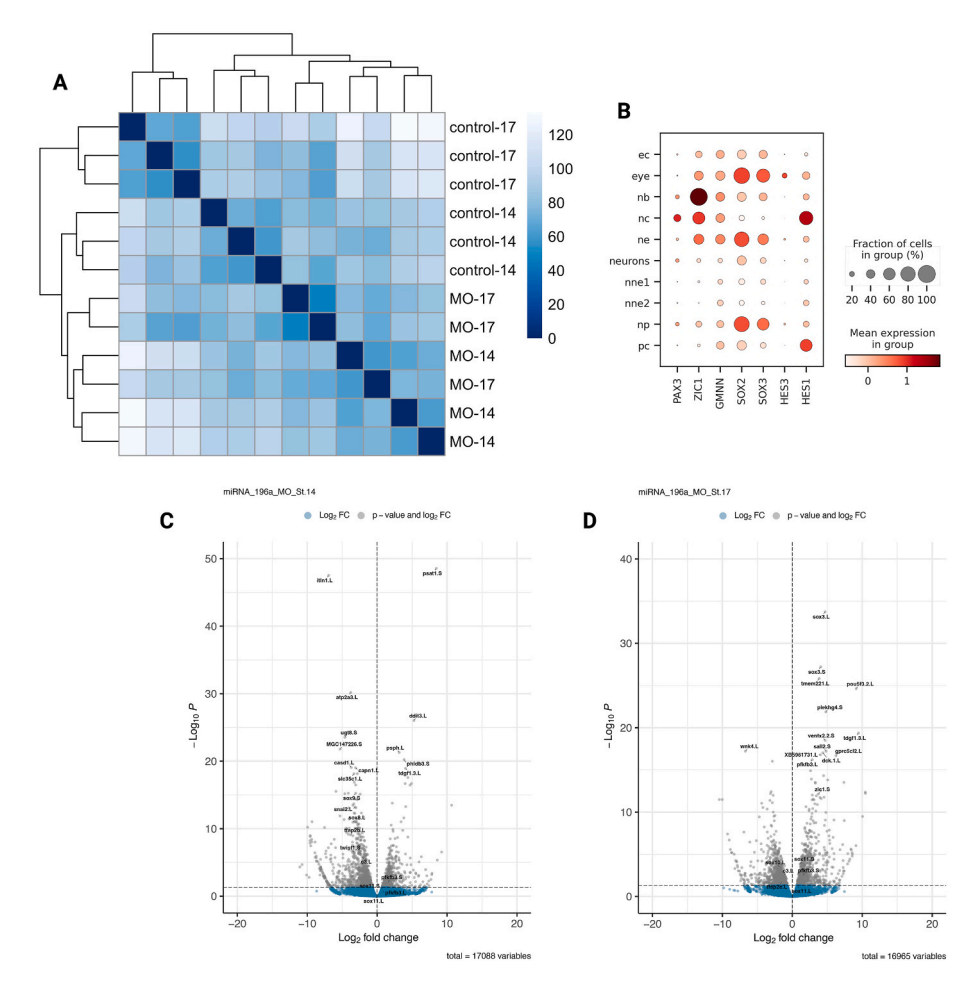


Fig. 4. Main features of RNA sequencing of neural border and neural crest after depletion of miR-196a. (A) Heatmap showing clustering of control and miR-196a KD samples. (B) Dotplot of NPB, neural and NC gene expression across tissues. Ec, ectoderm; nb, neural plate border; nc, neural crest; ne, neuroectoderm; nne, non-neural ectoderm; np, neural plate; pc, placode. (C–D) Volcano plots of differentially expressed genes follow miR-196a MO KD at stage14 (C) and stage17 (D).

neural border were misexpressed in various manners at both stages: *zic1* or *hes4* (*hairy2a*) expression was increased while early *msx1/2* expression and *tfap2b*, c and e levels were decreased. Such desequilibrium is known to lead to failure of neural crest induction. Indeed, NC specifiers *snai1/2*, *sox8*, *myc*, *foxd3*, *ets1*, and the EMT/migration marker matrix metalloprotease, *mmp28*, were not activated in morphant NC cells at either stage. The same profile was observed for cranial placode markers *six1/4*, *eya1*, *pax8* and specified NNE markers *gata2/3*, and ectoderm differentiation marker *keratin*. This indicates that the three NB fates, NC, NNE and placodes, which should be clearly identified from NB explants at stage 14 (Kotov et al., 2024) are not observed in miR196a morphant NB. In contrast, early neural development (*sox2/3*, *zic2/3/4*) and pluripotency gene Oct4 orthologs (*pou5f3.1/2/3*) were highly expressed in NB ectoderm as well as in pre-migratory NC cells.

As BMP signalling balance is critical for dorsal ectoderm patterning, we were puzzled to observe chordin (*chrd*) expression in those explants, which do not contain mesoderm as confirmed prior to sequencing by checking for mesoderm genes. Chordin, however, is expressed in the floor plate neuroectoderm, which shares common embryonic origins with the notochord during gastrulation (the chordoneural hinge, Catala et al., 1996). This expression thus must be controlled negatively in other ectoderm area during normal development. Our observation indicates that upon KD of miR196a, BMP antagonist Chordin expression is potentially upregulated in the NB progenitors, creating a lower BMP signalling level than the one required for NB patterning (Alkobtawi et al., 2021). By itself, this result could explain the set of ectoderm patterning defects observed, with enlarged immature neural tissue and

loss of NB derivatives.

Furthermore, pluripotency factors (ventx2.2, pou5f31/2/3), neural stemness genes such as Sall3 (Kuroda et al., 2019) and Notch signalling effectors (hes3/4/5/1) regulate the balance between progenitor state and differentiation (Nichane et al., 2008a, 2008b). Depletion of mir-196a led to maintained expression of these genes in the NB and NC tissues during neurulation, in agreement with the expression patterns observed in toto (Figs. 2 and 3). Last, anterior-posterior patterning of the NC, as well as of the adjacent neural tube, is largely regulated by hox genes posterior to the mid-hindbrain boundary. In the morphant NB explants, which include both anterior and posterior ectoderm, increased hox gene expression is observed compared to control tissue. However, in the stage 17 pre-migratory NC explants, which normally include both anterior hox-negative cells and hoxa-b-c-d1/2/3-positive rhombencephalic cells, miR-196a depletion eliminated hox expression in the morphant tissue (Fig. 5, Fig. S6). It remains unclear, at this tissue resolution if this is due to loss of NC cells, or to their transformation into a mis patterned immature neural progenitor state.

Among the genes mis-regulated in morphant tissue, we hypothesized that some might be direct miRNA targets, which should be upregulated upon miRNA depletion, while others could be affected indirectly. We collated genes which are predicted to be miR-196a targets, using miRanda with default settings, (John et al., 2004). These include NC genes sox10, hand1 and Hox genes hoxc8, hoxd8, hoxb3, hoxb6 and neural and ectoderm gene pax2, and placodal gene eya1 (Table 2). To directly validate this potential regulation $in\ vivo\ during\ ectoderm\ patterning, we then tested in toto expression of <math>sox10$ in unilateral

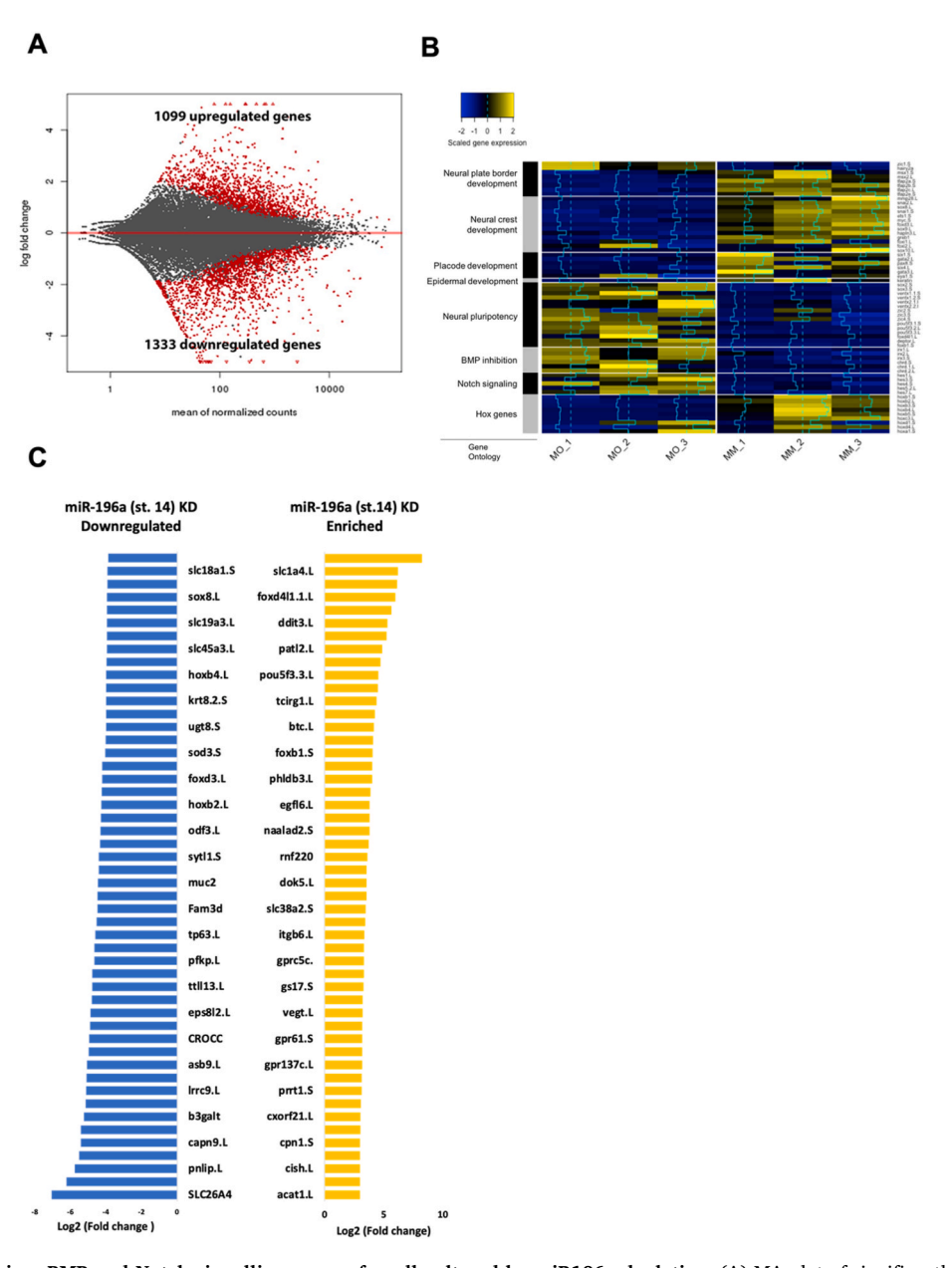


Fig. 5. Ectoderm patterning, BMP and Notch signalling are profoundly altered by miR196a depletion. (A) MA plot of significantly differentially expressed genes in RNA-seq data following miR-196a KD (stage 14). (B) Heatmap for selected differentially expressed genes (miR-196a MO vs miR-196a MM). Colour depicts gene expression where yellow represents overexpression and blue under expression. The blue line running throughout the boxes is a histogram representing the level of either upregulation or downregulation against the dotted midline (no change). (C) Top 50 enriched and depleted significantly differentially expressed genes following miR-196a MO KD at stage14. (For interpretation of the references to colour in this figure legend, the reader is referred to the Web version of this article.)

miR-196a KD and rescue injections (Fig. 2). The expression of sox10 was reduced after MO KD and rescued upon co-injection with miRNA mimic. However, we did observe a striking expansion for the neural and placode marker sox11, encompassing the entire dorsal ectoderm and consistent with the morphant patterns described above (Fig. S3C). Sox11 is not a direct target of miR-196a in Xenopus, however it was found to be a target in humans when analysis TargetScan database. In future annotations of Xenopus genomes, it would be worth revisiting this as we found sox11 to be enriched following miR-196a KD in our RNA-seq data. This analysis confirms that some direct targets for miR-196a are tightly controlled during vertebrate embryo ectoderm, neural and NB patterning.

Overexpression of miR-196a has been shown to cause eye defects in *Xenopus* embryos (Qiu et al., 2009). Work aiming to investigate miR-196a further identified anterior neural development phenotypes (Gessert et al., 2010). Therefore, it was expected that following

misexpression of miR-196a with MO or miRNA mimic that there would be phenotypes generated on eye markers and neural markers. As expected, the neural marker Pax6, responsible in eye development (Grocott et al., 2020), is enriched after miR-196a KD. Interestingly the skeletal preparations for miR-196a KD tadpoles showed craniofacial defects (Fig. 1), indicative of abnormal NC specification, this has also been seen in previous work by Gessert and colleagues (Gessert et al., 2010) and our own miR-196a CRISPR knockouts (Godden et al., 2021).

3. Conclusion

Collectively, our findings highlight the essential role of miR-196a in patterning to dorsal ectoderm of the vertebrate embryo model *Xenopus laevis*. At the NP stage, when the different ectodermal fates are established, miR-196a activity controls the expression of more than 2,400

Table 2
Results of miRanda analysis for miR-196a. Contents cover Gene ID, name and predicted binding of miR-196a (query) and 3' UTR of gene (Ref), with miRanda score in last column, higher score indicates stronger match.

Gene ID	Gene name	Full gene name	Predicted binding miRanda	miRanda score
ENSXETT00000013902	sox10	SRY-box 10	Query: 3' ggUUGUUGUACUUUGAUGGAu 5' : : Ref: 5' aaAGCAGCTTG–ACTACTTa 3'	140
ENSXETT00000018548	hand1	heart and neural crest derivatives expressed 1	Query: 3' ggUUG-UUGUACUUUGAUGGAu 5' : : : Ref: 5' acAGCAAACGTGTGACTACCTa 3'	166
ENSXETT00000031060	pax2	paired box 2	Query: 3' ggUUGUUGUACUUUGAUGgau 5' Ref: 5' gaAACCACATGAAACTACagg 3'	147
ENSXETT00000069246	eya1	EYA transcriptional coactivator and phosphatase $\boldsymbol{1}$	Query: 3' ggUUGUUGUACUUUGAUGGAu 5' : : : Ref: 5' aaGATAAACTG-GACTACCTa 3'	153
ENSXETT00000050682	hoxc8	Homeobox C8	Query: 3' ggUUGUUGUACUUUGAUGGAu 5' : Ref: 5' ccAACAAC-TAAAACTGCCTa 3'	157
ENSXETT00000070016	hoxd8	Homeobox D8	Query: 3' ggUUGUUGUAC-U-UUGAUGGAu 5' :: : Ref: 5' tcACCGGGGTGTATAACTACCTa 3'	149
ENSXETT00000047547	hoxb3	Homeobox B3	Query: 3' ggUUGUUGUACUUUGAUGGAu 5' : Ref: 5' gaAGGAAGATGTAACTACCTa 3'	167
ENSXETT00000047588	hoxb6	Homeobox B6	Query: 3' ggUUGUU-GUACUUUGAUGGAu 5' : : Ref: 5' atGATAATCCTCCAACTACCTa 3'	154

genes. These include direct and indirect regulated genes. Depletion of miR196 was carefully controlled using mimic RNA oligonucleotides in vivo, an experimental strategy we previously developed for our CRISPR miRNA knockouts (Godden et al., 2021) and allows us to exclude compensatory action of the paralog miR-196b. The main function of miR-196a seems to restrict neural fate in the dorsal ectoderm. When miR-196a is depleted, this results in failure to form other ectoderm derivatives such as NC and placodes and NNE. Some tissues, such as the hatching gland ectoderm forming at later neurula stage, independently of the initial dorsal ectoderm patterning, seemed unaffected or even slightly increased in the morphant context. These observations are consistent with sox2 expansion in miR-196a KD embryos (Fig. 3 and S3A) and could contribute towards the reduction in NC marker expression seen in Fig. 2; similar to previous observations in avian models suggesting that sox2 misexpression can inhibit NC formation (Hu et al., 2014; Wakamatsu et al., 2004).

Defective NC formation is not compensated for at later stages of development, while it seems that other early defects in the non-NC tissues are transient since tadpole morphology is globally normal. *Sox10* depletion is known to lead to a rise in NC cell apoptosis and reduction in cell proliferation (Honore et al., 2003). *Snail2* is required for the induction of NC; and is anti-apoptotic (Klymkowsky et al., 2010; Shi et al., 2011). Additionally, we found cell cycle and regulatory markers: *cdc25b*, *cdc6*, *ccnb1* (*cyclin B1*) *ccnb3* (*cyclin B3*) in our RNA-seq data to be enriched following loss of miR-196a. Combined, this suggests that miR-196a KD, which reduced expression of *sox10* and *snail2* (Fig. 2), is disrupting proliferation, progression and maintenance of a pool of NC cells, which is potentially leading to the craniofacial deformation seen later in development (Fig. 1C). To validate this further apoptosis assays like Tunel assays would explain if cells were going through apoptosis or being held.

The second major function of miR-196a is to repress expression of

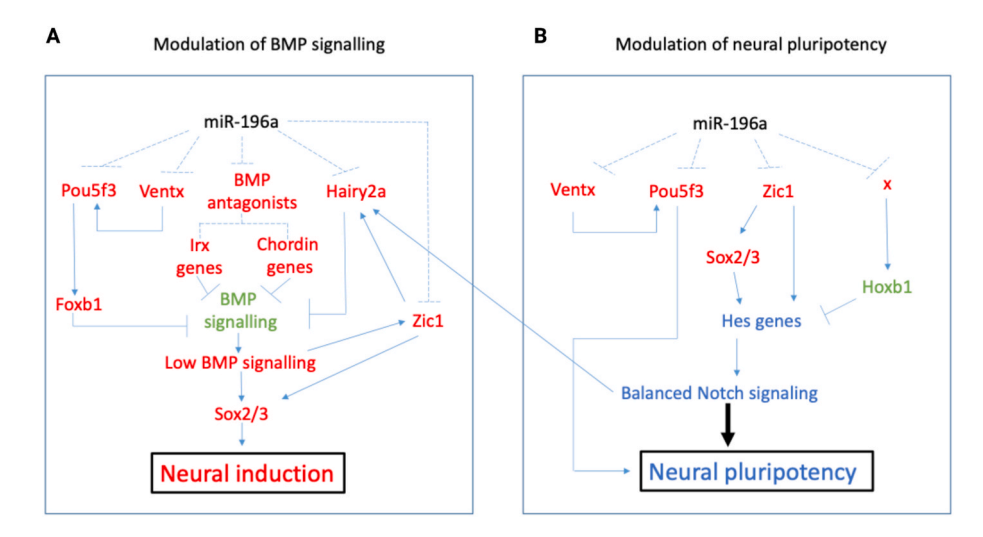


Fig. 6. Model of the potential molecular mechanisms miR-196a uses to prevent neural induction (A) and control neural pluripotency (B) during Xenopus neuroectoderm patterning. Red represents repression, green represents expression and blue represents balanced. Solid and dashed lines are the verified and predicted regulatory relationships, respectively. (For interpretation of the references to colour in this figure legend, the reader is referred to the Web version of this article.)

pluripotency and neural stemness genes and allow the onset of neuronal differentiation in the central nervous system. We propose a working model (Fig. 6) to place miR-196a in the current neural/neural border/non-neural ectoderm gene regulatory network, and a rich resource of candidate genes for further validation of their functions in the initial steps of ectoderm regionalisation in vertebrates.

4. Materials and methods

4.1. Xenopus husbandry

All experiments were carried out in accordance with relevant laws and institutional guidelines at the University of East Anglia, with full ethical review and approval, compliant to UK Home Office regulations. To obtain *Xenopus laevis* embryos, females were primed with 100 units of PMSG and induced with 500 units of human chorionic gonadotrophin. Eggs were collected manually and fertilised *in vitro*. Embryos were dejellied in 2 % L-cysteine, incubated at 18 °C and microinjected in 3 % Ficoll into 1-cell at the 2/4-cell stage. Embryos were left to develop at 23 °C. Embryo staging is according to Nieuwkoop and Faber normal table of *Xenopus* development. GFP/LacZ capped mRNA for injections was prepared using the SP6 mMESSAGE mMACHINE kit, 50 pg were injected per embryo.

4.2. Embryo injection

Xenopus laevis embryos were used for all WISH (whole mount in situ hybridisation) experiments in this project. Embryos were injected using a 10 nL calibrated needle. MO dose was optimized to 60 ng for miRNAs; MO and GFP or lacZ capped mRNA were injected at 4 cell stage of embryo development into the right dorsal blastomere.

Xenopus laevis embryos were injected at the 4-cell stage of development into one dorsal blastomere with 300 pg GFP or lacZ plus MO, miRNA mimic or combination. Synthetic LNA miRNA mimic, complementary to the mature miRNA sequence (SFig. 3B). For all markers use of synthetic miRNA mimic were used to rescue phenotypes generated by miRNA MO KD. Use of miRNA mimic and control mimic cel-miR-39-3p alone saw no impact on embryo development. Rescue of the miRNAs is specific with use of relevant synthetic miRNA (Supp Fig. 3). MiRNA expression levels were significantly increased and decreased following use of miRNA mimic, and MO. When used together miRNA mimic rescues decreased expression levels by miRNA MO (Fig. S3).

MiRCURY LNA miRNA mimics were used to replace miRNA in MO miRNA KD rescue. For miR-196a: (Qiagen, 339173 YM00470616-ADA, MIMAT0000226); hsa-miR-196a-5p compatible with xtr-miR-196a sequence: 5' UAGGUAGUUUCAUGUUGUUGGG. A negative control miRNA mimic recommended by Qiagen was used (Qiagen, 331973 YM00479902-ADA); Negative control (cel-miR-39-3p), sequence 5'UCACCGGGUGUAAAUCAGCUUG.

Chi-squared test for association was used to test phenotype yes or no categories for MO injected embryos to see if there was a relationship between two categorical values. Excel was used to collate and tabulate data. IBM SPSS v25 to carry out Chi-squared test. When describing statistical significance; $p<0.05=\ast,\,p<0.01=\ast\ast,\,p<0.001=\ast\ast\ast,\,p=<0.0001=\ast\ast\ast\ast$

4.3. RT-qPCR

Embryos were frozen on dry ice before RNA extraction. Total RNA was extracted from five stage14 *Xenopus tropicalis* embryos. Embryos were homogenised with a micro pestle and RNA was extracted according to manufacturer's guidance, Quick-RNA Mini prep plus kit (Zymo, Cat no. R1058). Samples were eluted in 25 μL of nuclease free water; RNA concentration and purity quantified on a Nanodrop 1000 and 1 μL was checked on a 2 % agarose gel.

To produce cDNA for q-RT-PCR, miRCURY LNA RT kit was used

(Qiagen, Cat No./ID: 339340). To generate cDNA 50 ng of RNA was used. cDNA was produced on a thermocycler with the following programme: 42 $^{\circ}$ C for 60 min and 95 $^{\circ}$ C for 5 min cDNA was diluted 1:40 for q-RT-PCR. cDNA was stored at -20 $^{\circ}$ C. qRT-PCR reactions were set up in 10 μ L volume containing 4 μ L cDNA, 1 μ L primer (in accordance with manufacturer dilute for Qiagen LNA miRNA primer), and 5 μ L Sybr-Green (Applied Biosystems 4309155). Primers for q-RT-PCR sequences were the following: xtr-miR-196a 5' – UAGGUAGUUUCAUGUUGG – 3' (Qiagen, YP02103491), xtr-miR-196b 5'- UAGGUAGUUUUAU-GUUGUUGG – 3' (Qiagen, YP02104328), and U6 snRNA 5'-CTCGCTTCGGCAGCACA – 3'.

4.4. In situ hybridization

WISH with LNA probes was carried out according to (Ahmed et al., 2015; Antonaci et al., 2023; Sweetman et al., 2006) Other WISH and probe synthesis were carried out according to (Monsoro-Burq, 2007; Sive et al., 2007). All *in situ* experiments where graphs are included were conducted with a minimum of biological triplicate with different maternal and paternal Xenopus, n numbers indicate the total number of embryos in the experimental group and bars in the bar chart indicate percentage of embryos displaying normal or abnormal phenotypes.

4.5. RNA sequencing

For RNA-sequencing embryos were injected into one blastomere at 4-cell stage with one of two MO's (miR-196a or miR-196a mismatch (MM)) into one dorsal blastomere to target neural and NC tissue in one side of the embryo. Embryos were left to develop until stage 14 or 17. One group of embryos underwent WISH to check NC that genes were knocked down (We include representative images from separate experiments in Fig. S5) and the other group underwent NC dissections and RNA extraction. Three replicates were collected for each condition (MO, MM, and non-injected control). RNA samples underwent quality control using Bioanalyzer (Agilent) and RT-qPCR was used to further validate the KD of NC-specific genes in MO-injected samples (Godden et al., 2021). Triplicates were then processed to Illumina HiSeq 2500RNA sequencing after unstranded library preparation (50bp paired-end sequencing on the HiSeq High Output run mode PE100 for sequencing.

4.6. Data analysis

RNA-sequencing reads were mapped to the *Xenopus laevis* v10.1 genome assembly using STAR (v.2.7.3a), (Dobin et al., 2013). Differential expression analysis was carried out using DESeq2 (v.1.32.0) (Love et al., 2014), in R (v.4.1.1). Genes with an adjusted *p*-value below 0.05–0.15 were considered significant and were reported by the workflow. The gene model used in the DE bioinformatic analysis was *Xenopus laevis* (NCBI v10.1). For GO enrichment analysis of a DE genes we used ClusterProfiler (v.4.0.5). MiRanda was used to analyse miRNA-196a 3' UTR gene targets with default settings (John et al., 2004). Mature miRNA sequences were accessed from miRbase (Griffiths-Jones et al., 2006), and annotation and reference fasta file accessed from Ensembl v106 *Xenopus tropicalis* v9.1 genome as miR-196a, b are not annotated in the *Xenopus laevis* genome, but is highly conserved. RNA-sequencing data is available at GEO under accession number: GSE289705 (under embargo until acceptance for publication).

4.7. Alcian blue craniofacial cartilage staining

Stage 45 Tadpoles were dehydrated in ethanol and were then left in Alcian blue (20 mg) for 3 nights. After this, embryos were washed 3 times for 15 min in 95 % ethanol (Sigma, UK) then rehydrated in 2 % KOH using 10-min washes of 75 % ethanol in 2 % KOH, 50 % ethanol in 2 % KOH, 25 % ethanol in 2 % KOH then 3×2 % KOH washes. Embryos were then stored in glycerol with 1-h washes of 20 % glycerol in 2 %, 40

% glycerol in 2 % KOH, 60 % glycerol in 2 % KOH and finally stored in 80 % glycerol in 2 % KOH. Embryos were washed 3 times for 5 min in PBS before 20 min incubation in 10 mL pre-incubation solution (0.5 X SSC (150 mM NaCl, 15 mM sodium citrate, pH 7.2), 0.1 % Tween. 20), and then embryos were incubated in 10 mL of depigmentation solution (5 % formamide, 0.5 X SSC, 3 % H2O2). Embryos were then carefully dissected under a microscope using fine forceps to remove outermost ectoderm and mesenchyme surrounding craniofacial cartilage. Method for this clearing was based on (Affaticati et al., 2018).

Embryos were imaged on agarose dishes with a Zeiss Axiovert Stemi SV 11, Jenoptik ProgRes C5 camera (Germany), ProgRes software version 2.7.6. Fluorescent images were captured using Leica MZ 16 F microscope, Leica DFC300 FX camera, Leica Kubler codix light source, Leica FireCam software version 3.4.1. Figures were created using Adobe Photoshop and BioRender.com.

CRediT authorship contribution statement

Alice M. Godden: Writing – review & editing, Writing – original draft, Visualization, Validation, Resources, Project administration, Methodology, Investigation, Formal analysis, Data curation. Nicole Ward: Visualization, Validation, Resources, Methodology, Investigation, Formal analysis. Méghane Sittewelle: Visualization, Validation, Methodology, Investigation. Marco Antonaci: Validation, Methodology, Investigation. Rafeeq Mir: Investigation. Aleksandr Kotov: Software, Formal analysis, Data curation. Anne H. Monsoro-Burq: Writing – review & editing, Writing – original draft, Visualization, Validation, Supervision, Resources, Methodology, Investigation, Formal analysis, Data curation, Conceptualization. Grant N. Wheeler: Writing – review & editing, Writing – original draft, Visualization, Validation, Supervision, Resources, Project administration, Methodology, Investigation, Funding acquisition, Formal analysis, Data curation, Conceptualization.

Acknowledgements

We would like to thank Prof. Saint-Jeannet and Dr. Walmsley for plasmids, Prof. Münsterberg and Dr. Simon Moxon for helpful discussions and the Wheeler, Münsterberg, and Monsoro-Burq labs for support. We would also like to thank Johannes Wittig for drafting Fig. 1A.

This work was supported by the UKRI Biotechnology and Biological Sciences Research Council Norwich Research Park Biosciences Doctoral Training Partnership (Grant numbers BB/M011216/1 to GW/AG and BB/J014524/1 to NW/GW). This project also received funding from BBSRC project grant no. BB/W017032 to RM/GW, European Union Horizon 2020 Marie Skłodowska-Curie grant no. 860635, NEUcrest ITN (AK, MA, AHMB, GW); Agence Nationale pour la Recherche ANR-15-CE13-0012-01, ANR- 21-CE13-0028; Institut Universitaire de France (AHMB); Fondation pour la Recherche Médicale (AHMB). RNA sequencing used the ICGex NGS platform of Institut Curie (ANR-10-EQPX-03; ANR-10-INBS-09-08; Canceropole Ile-de-France; SiRIC-Curie INCa-DGOS-4654).

Appendix A. Supplementary data

Supplementary data to this article can be found online at $\frac{https:}{doi.}$ org/10.1016/j.ydbio.2025.09.007.

Data availability

Data will be made available on request.

References

Affaticati, P., Le Mevel, S., Jenett, A., Riviere, L., Machado, E., Mughal, B.B., Fini, J.B., 2018. X-FaCT: Xenopus-fast clearing technique. Methods Mol. Biol. 1865, 233–241. Ahmed, A., Ward, N.J., Moxon, S., Lopez-Gomollon, S., Viaut, C., Tomlinson, M.L., Patrushev, I., Gilchrist, M.J., Dalmay, T., Dotlic, D., Munsterberg, A.E., Wheeler, G.

- N., 2015. A database of microRNA expression patterns in Xenopus laevis. PLoS One 10, e0138313.
- Alberti, C., Cochella, L., 2017. A framework for understanding the roles of miRNAs in animal development. Development 144, 2548–2559.
- Alkobtawi, M., Pla, P., Monsoro-Burq, A.H., 2021. BMP signaling is enhanced intracellularly by FHL3 controlling WNT-dependent spatiotemporal emergence of the neural crest. Cell Rep. 35, 109289.
- Antonaci, M., Godden, A.M., Wheeler, G.N., 2023. Determining miRNA expression patterns in xenopus. Methods Mol. Biol. 2630, 145–154.
- Antonaci, M., Wheeler, G.N., 2022. MicroRNAs in neural crest development and neurocristopathies. Biochem. Soc. Trans. 50, 965–974.
- Aoto, K., Sandell, L.L., Butler Tjaden, N.E., Yuen, K.C., Watt, K.E., Black, B.L., Durnin, M., Trainor, P.A., 2015. Mef2c-F10N enhancer driven beta-galactosidase (LacZ) and Cre recombinase mice facilitate analyses of gene function and lineage fate in neural crest cells. Dev. Biol. 402, 3–16.
- Bachetti, T., Bagnasco, S., Piumelli, R., Palmieri, A., Ceccherini, I., 2021. A common 3'UTR variant of the PHOX2B gene is associated with infant life-threatening and sudden death events in the Italian population. Front. Neurol. 12, 642735.
- Bartel, D.P., 2004. MicroRNAs: genomics, biogenesis, mechanism, and function. Cell 116, 281–297
- Betancur, P., Bronner-Fraser, M., Sauka-Spengler, T., 2010. Assembling neural crest regulatory circuits into a gene regulatory network. Annu. Rev. Cell Dev. Biol. 26, 581–603.
- Bhattacharya, D., Rothstein, M., Azambuja, A.P., Simoes-Costa, M., 2018. Control of neural crest multipotency by Wnt signaling and the Lin28/let-7 axis. eLife 7.
- Catala, M., Teillet, M., DeRobertis, E., LeDouarin, N., 1996. A spinal cord fate map in the avian embryos: while regressing, Hensen's node lays down the notochord and floor plate thus joining the spinal cord lateral walls. Development 122, 2599–2610.
- Chandra, S., Vimal, D., Sharma, D., Rai, V., Gupta, S.C., Chowdhuri, D.K., 2017. Role of miRNAs in development and disease: lessons learnt from small organisms. Life Sci. 185, 8–14.
- Cheung, M., Briscoe, J., 2003. Neural crest development is regulated by the transcription factor Sox9. Development 130, 5681–5693.
- Copeland, J., Simoes-Costa, M., 2020. Post-transcriptional tuning of FGF signaling mediates neural crest induction. Proc. Natl. Acad. Sci. U. S. A. 117, 33305–33316.
- de Croze, N., Maczkowiak, F., Monsoro-Burq, A.H., 2011. Reiterative AP2a activity controls sequential steps in the neural crest gene regulatory network. Proc. Natl. Acad. Sci. U. S. A. 108, 155–160.
- Dobin, A., Davis, C.A., Schlesinger, F., Drenkow, J., Zaleski, C., Jha, S., Batut, P., Chaisson, M., Gingeras, T.R., 2013. STAR: ultrafast universal RNA-seq aligner. Bioinformatics 29, 15–21.
- Evsen, L., Li, X., Zhang, S., Razin, S., Doetzlhofer, A., 2020. let-7 miRNAs inhibit CHD7 expression and control auditory-sensory progenitor cell behavior in the developing inner ear. Development 147.
- Figueiredo, A.L., Maczkowiak, F., Borday, C., Pla, P., Sittewelle, M., Pegoraro, C., Monsoro-Burq, A.H., 2017. PFKFB4 control of AKT signaling is essential for premigratory and migratory neural crest formation. Development 144, 4183–4194.
- Flynt, A.S., Rao, M., Patton, J.G., 2017. Blocking zebrafish MicroRNAs with morpholinos. Methods Mol. Biol. 1565, 59–78.
- Friedman, R.C., Farh, K.K., Burge, C.B., Bartel, D.P., 2009. Most mammalian mRNAs are conserved targets of microRNAs. Genome Res. 19, 92–105.
- Gessert, S., Bugner, V., Tecza, A., Pinker, M., Kuhl, M., 2010. FMR1/FXR1 and the miRNA pathway are required for eye and neural crest development. Dev. Biol. 341, 222–235.
- Godden, A.M., Antonaci, M., Ward, N.J., van der Lee, M., Abu-Daya, A., Guille, M., Wheeler, G.N., 2021. An efficient miRNA knockout approach using CRISPR-Cas9 in xenopus. Dev. Biol. 483, 66–75.
- Godden, A.M., Antonaci, M., Wheeler, G.N., 2023. An efficient CRISPR-Cas9 method to knock out MiRNA expression in Xenopus tropicalis. Methods Mol. Biol. 2630, 231–241
- Gouignard, N., Maccarana, M., Strate, I., von Stedingk, K., Malmstrom, A., Pera, E.M., 2016. Musculocontractural Ehlers-Danlos syndrome and neurocristopathies: dermatan sulfate is required for xenopus neural crest cells to migrate and adhere to fibronectin. Dis. Model. Mech. 9, 607–620.
- Griffiths-Jones, S., Grocock, R.J., van Dongen, S., Bateman, A., Enright, A.J., 2006. miRBase: microRNA sequences, targets and gene nomenclature. Nucleic Acids Res. 34, D140–D144.
- Grocott, T., Lozano-Velasco, E., Mok, G.F., Munsterberg, A.E., 2020. The Pax6 master control gene initiates spontaneous retinal development via a self-organising turing network. Development 147.
- Honore, S.M., Aybar, M.J., Mayor, R., 2003. Sox10 is required for the early development of the prospective neural crest in xenopus embryos. Dev. Biol. 260, 79–96.
- Hu, N., Strobl-Mazzulla, P.H., Simoes-Costa, M., Sanchez-Vasquez, E., Bronner, M.E., 2014. DNA methyltransferase 3B regulates duration of neural crest production via repression of Sox10. Proc. Natl. Acad. Sci. U. S. A. 111, 17911–17916.
- John, B., Enright, A.J., Aravin, A., Tuschl, T., Sander, C., Marks, D.S., 2004. Human MicroRNA targets. PLoS Biol. 2, e363.
- Klymkowsky, M.W., Rossi, C.C., Artinger, K.B., 2010. Mechanisms driving neural crest induction and migration in the zebrafish and Xenopus laevis. Cell Adhes. Migrat. 4, 595–608.
- Kotov, A., Seal, S., Alkobtawi, M., Kappes, V., Ruiz, S.M., Arbes, H., Harland, R.M., Peshkin, L., Monsoro-Burq, A.H., 2024. A time-resolved single-cell roadmap of the logic driving anterior neural crest diversification from neural border to migration stages. Proc. Natl. Acad. Sci. U. S. A. 121, e2311685121.

- Kuroda, T., Yasuda, S., Tachi, S., Matsuyama, S., Kusakawa, S., Tano, K., Miura, T., Matsuyama, A., Sato, Y., 2019. SALL3 expression balance underlies lineage biases in human induced pluripotent stem cell differentiation. Nat. Commun. 10, 2175.
- human induced pluripotent stem cell differentiation. Nat. Commun. 10, 2175.
 Lee, R.C., Feinbaum, R.L., Ambros, V., 1993. The C. elegans heterochronic gene lin-4 encodes small RNAs with antisense complementarity to lin-14. Cell 75, 843–854.
- Lewis, M.A., Steel, K.P., 2010. MicroRNAs in mouse development and disease. Semin. Cell Dev. Biol. 21, 774–780.
- Love, M.I., Huber, W., Anders, S., 2014. Moderated estimation of fold change and dispersion for RNA-seq data with DESeq2. Genome Biol. 15, 550.
- Milet, C., Maczkowiak, F., Roche, D.D., Monsoro-Burq, A.H., 2013. Pax3 and Zic1 drive induction and differentiation of multipotent, migratory, and functional neural crest in xenopus embryos. Proc. Natl. Acad. Sci. U. S. A. 110, 5528–5533.
- Mok, G.F., Lozano-Velasco, E., Munsterberg, A., 2017. microRNAs in skeletal muscle development. Semin. Cell Dev. Biol. 72, 67–76.
- Monsoro-Burq, A.H., 2007. A rapid protocol for whole-mount in situ hybridization on xenopus embryos. CSH Protoc 2007 pdb prot4809.
- Nichane, M., de Croze, N., Ren, X., Souopgui, J., Monsoro-Burq, A.H., Bellefroid, E.J., 2008a. Hairy2-Id3 interactions play an essential role in xenopus neural crest progenitor specification. Dev. Biol. 322, 355–367.
- Nichane, M., Ren, X., Souopgui, J., Bellefroid, E.J., 2008b. Hairy2 functions through both DNA-binding and non DNA-binding mechanisms at the neural plate border in xenopus. Dev. Biol. 322, 368–380.
- Petrova, K., Tretiakov, M., Kotov, A., Monsoro-Burq, A.H., Peshkin, L., 2024. A new atlas to study embryonic cell types in xenopus. Dev. Biol. 511, 76–83.
- Pilon, N., 2021. Treatment and prevention of neurocristopathies. Trends Mol. Med. 27, 451–468.
- Pla, P., Monsoro-Burq, A.H., 2018. The neural border: induction, specification and maturation of the territory that generates neural crest cells. Dev. Biol. 444 (Suppl. 1), \$36,546
- Plouhinec, J.L., Medina-Ruiz, S., Borday, C., Bernard, E., Vert, J.P., Eisen, M.B., Harland, R.M., Monsoro-Burq, A.H., 2017. A molecular atlas of the developing ectoderm defines neural, neural crest, placode, and nonneural progenitor identity in vertebrates. PLoS Biol. 15, e2004045.

- Qiu, R., Liu, Y., Wu, J.Y., Liu, K., Mo, W., He, R., 2009. Misexpression of miR-196a induces eye anomaly in Xenopus laevis. Brain Res. Bull. 79, 26–31.
- Salim, U., Kumar, A., Kulshreshtha, R., Vivekanandan, P., 2022. Biogenesis,
- characterization, and functions of mirtrons. Wiley Interdiscip Rev RNA 13, e1680. Sauka-Spengler, T., Bronner-Fraser, M., 2008. A gene regulatory network orchestrates neural crest formation. Nat. Rev. Mol. Cell Biol. 9, 557–568.
- Scerbo, P., Monsoro-Burq, A.H., 2020. The vertebrate-specific VENTX/NANOG gene empowers neural crest with ectomesenchyme potential. Sci. Adv. 6, eaaz1469.
- Schoen, C., Aschrafi, A., Thonissen, M., Poelmans, G., Von den Hoff, J.W., Carels, C.E.L., 2017. MicroRNAs in palatogenesis and cleft palate. Front. Physiol. 8, 165.
- Shah, V.V., Soibam, B., Ritter, R.A., Benham, A., Oomen, J., Sater, A.K., 2017. MicroRNAs and ectodermal specification I. Identification of miRs and miR-targeted mRNAs in early anterior neural and epidermal ectoderm. Dev. Biol. 426, 200–210.
- Shi, J., Severson, C., Yang, J., Wedlich, D., Klymkowsky, M.W., 2011. Snail2 controls mesodermal BMP/Wnt induction of neural crest. Development 138, 3135–3145.
- Sive, H.L., Grainger, R.M., Harland, R.M., 2007. Synthesis and purification of digoxigenin-labeled RNA probes for in situ hybridization. CSH Protoc 2007, pdb prot4778. https://doi.org/10.1101/pdb.prot4778.
- Steventon, B., Mayor, R., 2012. Early neural crest induction requires an initial inhibition of Wnt signals. Dev. Biol. 365, 196–207.
- Sweetman, D., Rathjen, T., Jefferson, M., Wheeler, G., Smith, T.G., Wheeler, G.N., Munsterberg, A., Dalmay, T., 2006. FGF-4 signaling is involved in mir-206 expression in developing somites of chicken embryos. Dev. Dyn. 235, 2185–2191.
- Thatcher, E.J., Bond, J., Paydar, I., Patton, J.G., 2008. Genomic organization of zebrafish microRNAs. BMC Genom. 9, 253.
- Wakamatsu, Y., Endo, Y., Osumi, N., Weston, J.A., 2004. Multiple roles of Sox2, an HMG-box transcription factor in avian neural crest development. Dev. Dyn. 229, 74–86.
- Ward, N.J., Green, D., Higgins, J., Dalmay, T., Munsterberg, A., Moxon, S., Wheeler, G. N., 2018. microRNAs associated with early neural crest development in Xenopus laevis. BMC Genom. 19, 59.
- Weiner, A.M.J., 2018. MicroRNAs and the neural crest: from induction to differentiation. Mech. Dev. 154, 98–106.
- Yapijakis, C., 2020. Regulatory role of MicroRNAs in brain development and function. Adv. Exp. Med. Biol. 1195, 237–247.